

Shape Optimization of Plate and Shell Structures

M. E. Botkin*

General Motors Research Laboratories, Warren, Mich.

In the past, much of the work done in structural optimization consisted of resizing the members of fixed configuration models. There is, however, a broad class of plate and shell problems in which an additional reduction in mass can be attained by including in the design process the capability for varying the shape of boundaries and the shape and location of cutouts. This additional capability has made it necessary to address other problems such as how to maintain an adequate finite element model, how to define perfectly general shapes which satisfy a number of criteria, and how to impose the proper constraints so that a realistic design results. The shape design capability is demonstrated on practical problems which result in as much as 35% weight savings over a uniform thickness design with fixed boundaries.

Introduction

STRUCTURAL optimization, in the classical sense, has been considered to be the minimization of structural mass by varying member sizes and plate thicknesses of a model in which the geometry remains unchanged. It soon becomes apparent, however, that an additional mass reduction can be attained by including in the design process the ability to vary the structural geometry. This idea seems particularly appealing in the case of plate and shell designs with thickness as the only design variable in which no further mass reduction can be attained due to either a minimum gage requirement or a constant thickness requirement imposed by the manufacturing process. This reasoning has led to the shape design process described in this paper. The process consists of adding design variables which characterize either the shape of an exterior boundary or the shape and location of an interior cutout. These additions lead to the necessity of addressing other problems such as how to maintain an adequate finite element model, how to define perfectly general shapes which meet a number of criteria, and how to impose the proper constraints so that a realistic design results.

Recent work in shape design generally can be categorized as follows: 1) weight (or mass) minimization with stress constraints, and 2) stress minimization. In the first category, several authors¹⁻³ have presented similar papers in which two-dimensional isoparametric finite elements were coupled with penalty function optimization to design the shapes of a variety of dams, axisymmetric plates, and axisymmetric pressure vessels. Design variables were usually considered to be the coefficients of polynomials used to approximate the boundary shape. Emphasis was placed upon the need to make the solution process more efficient through the use of analytical techniques for obtaining derivatives and approximation techniques for representing stress constraints. In the second category, authors have presented techniques based upon mathematical programming for designing fillets and other two-dimensional curved boundaries where stress concentrations might occur.^{4,5} Quite obviously, the solution to this problem is similar to the weight reduction problem except that the weight is replaced by the stress as the objective function of the optimization problem. An optimality criterion is used by the authors in Ref. 6 to obtain optimum shape design of plates for the case of mean compliance of elastic structures of a nonlinear material. Schnack⁷ used a constant

tangential stress distribution criterion to obtain the optimum shape of load-free notch surfaces.

In general, none of the aforementioned authors have treated the general three-dimensional plate and shell problem nor have they emphasized the need for a uniformly applicable approach for maintaining mesh integrity. Furthermore, only stress constraints have been considered which greatly limits the types of problems that may be solved.

Problem Statement and Assumptions

The general problem to be dealt with in this paper is the minimization of structural mass while satisfying certain constraints placed upon stresses, displacements, and frequencies. The problem can be stated mathematically as:

Minimize

$$F=f(\alpha_j), \quad j=1,2,\dots,n \quad (1)$$

subject to

$$g_k(\alpha_j) \leq G_k, \quad k=1,2,\dots,m \quad (2)$$

in which n is the number of design variables, α_j the design variables, and m the number of behavior constraints. Both g and f are, in general, nonlinear functions. Limitations are also placed upon the range of the design variables and are referred to as side constraints. A general-purpose computer program⁸ was written to handle the problem stated in Eqs. (1) and (2). The program couples the mathematical programming technique of feasible directions⁹ with a general-purpose finite element program. Finite element types available are two-noded beams and three-noded plates that allow both stretching and bending deformations. The shape design capability has been included in the optimization program by adding to the existing design variables of plate thickness and beam cross-sectional dimensions, ones which control the shape of the boundaries of the finite element model.

A basic ingredient of the design process is the structural response derivative matrix taken with respect to the design variables. In the case of shape design, the boundary shape is always related to the nodal point locations through a function. The necessary derivatives, then, would be with respect to the nodal point coordinates and can be obtained by partial differentiation of the well-known static equilibrium equations, as follows¹⁰:

$$\frac{\partial \{u\}}{\partial x_j} = -[K]^{-1} \sum_i \frac{\partial [K]_i}{\partial x_j} \{e\}_i \quad (3)$$

Presented as Paper 81-0553 at the AIAA/ASME/ASCE/AHS 22nd Structures, Structural Dynamics and Materials Conference, Atlanta, Ga., April 6-8, 1981; submitted April 13, 1981; revision received July 27, 1981. Copyright © American Institute of Aeronautics and Astronautics, Inc., 1981. All rights reserved.

*Senior Research Engineer, Engineering Mechanics Department.

in which $\partial\{u\}/\partial x_j$ is the partial derivative of the displacements with respect to the nodal coordinates that are directly influenced by the shape design variables. $[K]_l^e$ is the element stiffness matrix for element l , and $\{e\}_l$ are the displacements of element l . All elements are included in the summation that are influenced by the corresponding shape design variable. The term $\partial[K]_l^e/\partial x_j$ is the partial derivative of the element stiffness matrix with respect to the nodal coordinates. An analytical formulation for this term is strongly dependent on the element type and, therefore, a more general approach was used in which the derivative is obtained using finite differences.

Design Variable Selection

As is the case in many optimization problems, some latitude exists in the choice of design variables. In beam design problems, for instance, thickness and section dimensions could be chosen as design variables or merely the moments of inertia. Each choice may have its own advantages. The choice of design variables changes the character of the problem by changing the degree of nonlinearity of the objective or constraint functions or by imposing additional, implicit side constraints.

One obvious choice of design variables for shape design would be the nodal coordinates of the boundary it is desired to vary. A major problem with this choice would be the resulting large number of design variables. The advantage, of course, would be the ability to obtain a general curved boundary, consistent with the finite element model, in which the structure is allowed to assume whatever shape is necessary to obtain the minimum weight. The problem with this generality is that an undesirable or impractical shape will most surely be produced.

In the technique described in this paper, the design variable is chosen to be the amplitude of a prescribed function, or the summation of several functions, which relates the nodal points along the boundary. This choice will result in a relatively small number of design variables and the final design will more likely be a desirable shape. Furthermore, this choice lends itself to some practical engineering problems in which the general shape may be known and only slight modifications in this shape may be required.

Shape Design Element

In order to be consistent with the existing optimization program, the concept of a plate or shell shape design element was formulated. The concept is merely for convenience in transferring information between the optimization phase of the design and the analysis phase. The characteristics of the design element are its volume, design variables, and constraints. Figure 1 represents what may be considered to be a shape design element. The element is defined by four boundaries which, in a general sense, are the design variables. To create a design model, several design elements must be used. A polar coordinate system has been implemented, curve **a** in Fig. 1, so that design variables describing closed interior

curves can be more easily handled. In order to allow more generality, any number of prescribed functions, $r(\theta)$ or $f(s)$ (Fig. 1, curve **b**), may be summed to obtain the final shape

$$F(s) = \alpha_1 f_1(s) + \alpha_2 f_2(s) + \dots + \alpha_n f_n(s) \quad (4)$$

in which α_n are the actual design variables used by the optimization process.

From the viewpoint of the finite element analysis, each design element is composed of a number of triangular membrane or bending elements connecting a series of nodal points. The nodal point locations have been computed based upon the value of the shape design variables determined at a design stage. The volume of the design element is merely the summation of the volume of all the finite elements contained in the design element. Only one stress constraint is assigned per design element and its value is the maximum of all the finite element stresses.

Mesh Generation

Several problems associated with shape design variables were resolved by using a regionalized mesh generation technique. This method automatically generates internal nodal point locations of only the points in an isolated region influenced by the specific boundary which has changed. It permits the reduction of stress constraints from one per finite element to one per region and provides for easy identification of the structural elements in the region. Also, an obvious advantage is the ability to quickly create a finite element model or to quickly change the degree of mesh refinement.

A two-dimensional mesh generation algorithm¹¹ was modified for creation of three-dimensional plate models. This technique requires the model to be divided into coarse quadrilateral regions composed of straight lines or quadratic curves. A straight edge requires the definition of two nodal points, whereas a curved edge requires the definition of three. Each region is then automatically subdivided into structural elements specified by the number of divisions desired in the two local coordinate directions. The internal nodal point locations are computed using isoparametric mapping

$$x = \sum_{i=1}^8 N_i(\beta, \eta) x_i \quad (5)$$

$$y = \sum_{i=1}^8 N_i(\beta, \eta) y_i \quad (6)$$

$$z = \sum_{i=1}^8 N_i(\beta, \eta) z_i \quad (7)$$

where x , y , and z are the global coordinates of a nodal point; x_i , y_i , and z_i are the coordinates of the points specifying the regional boundaries; β and η are the unmapped coordinates of the point ($-1 \leq \beta \leq 1$, $-1 \leq \eta \leq 1$); and N_i is a shape function¹² determined by the degree of curvature of the boundaries. A boundary can be entirely specified by three points and, therefore, N_i must be quadratic.

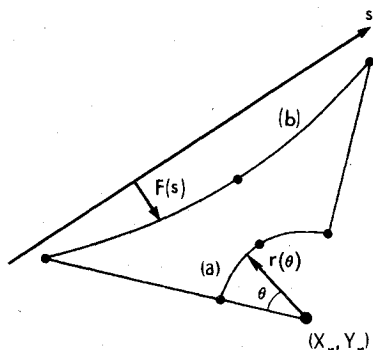


Fig. 1 Shape design element.

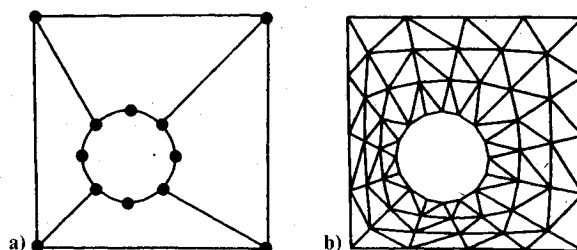


Fig. 2 a) Design element model; b) generated finite element model.

Table 1 Design results for plate example

Case	a_1	b_1	x_1	y_1	a_2	b_2	x_2	y_2	Mass, kg	Change, %
Initial	1.50	1.50	5.0	6.10	1.50	1.50	15.0	3.90	0.4371	0
A	1.88	1.88	5.0	6.10	1.42	1.42	15.0	3.90	0.4294	1.8
B	2.30	2.30	6.5	5.50	2.27	2.27	13.5	5.49	0.3939	9.9
C	3.00	2.40	6.00	5.47	3.00	2.40	14.00	5.47	0.3655	16.4
D	2.59	2.59	5.41	5.19	2.64	2.64	14.45	5.21	0.3091	29.3

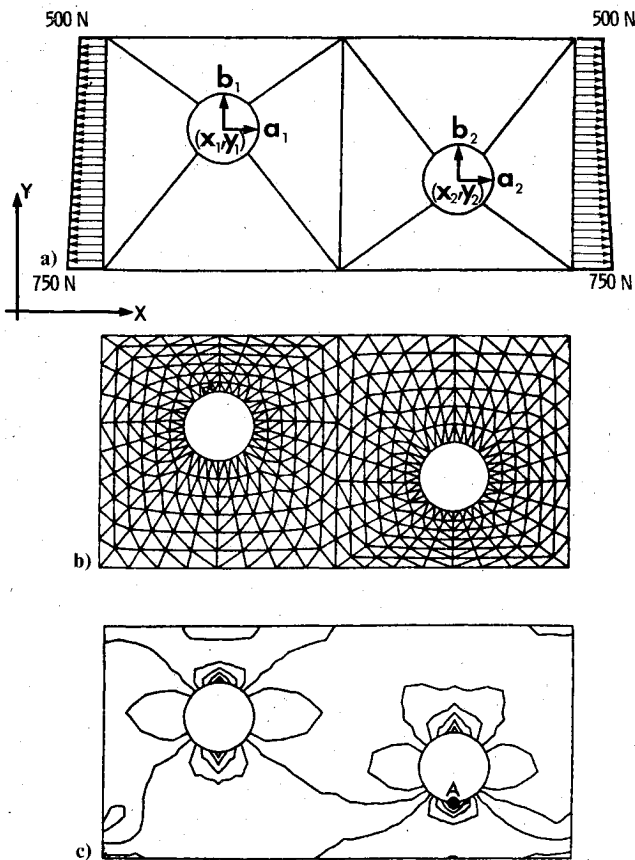


Fig. 3 a) Design element model; b) generated finite element mesh; c) stress contours.

Figure 2b shows an example of having used this technique to generate the mesh for the four shape design elements in Fig. 2a in which the curved boundary is reflected in the internal nodal point locations. The large dots in Fig. 2a represent the only nodal coordinates necessary for the definition of the boundaries. The actual location of these nodes is determined from the shape design variables. For instance, the radius and center location design variables associated with the circular hole determine the location of the nodes around the hole's boundary. As the design proceeds and the hole changes size and location, the internal node point locations are continuously updated relative to the nodes on the boundary. In the absence of such regeneration, the elements surrounding the boundary would soon become badly distorted.

The identification and computation of stress constraints has also been facilitated by using regionalized mesh generation. Generally, one stress constraint is assigned to each structural element. This results in a large number of constraints as well as a potential problem for shape design. As the shape changes, it is likely that the element which contains the maximum stress will also change, thus creating the possibility of having a different stress constraint being active at each step. By assigning one constraint per region and computing its value as the maximum of all the finite element stresses in the region, the jumping from one active constraint to another can be avoided. Even though by doing this one theoretically

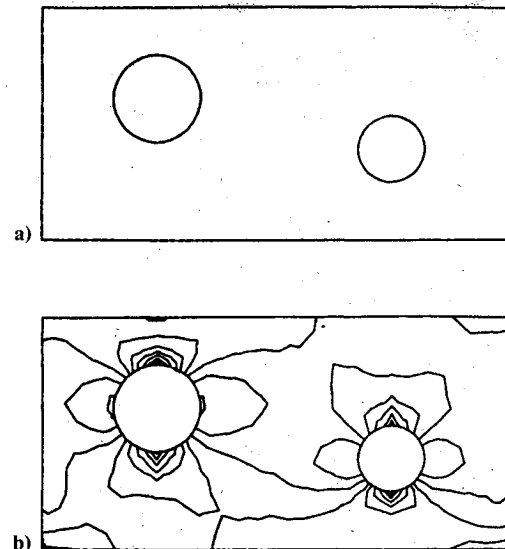


Fig. 4 a) Radius variables only, case A (mass = 0.4294 kg); b) stress contours, case A.

constructs a constraint function which is discontinuous and nondifferentiable, for the small boundary changes which occur from one step to the next the function behaved well and appeared to cause no problems. Another potential problem was if critical stresses occurred on more than one boundary of a design element. We monitored this condition by looking at stress contours in various stages of the design and, if this had occurred, an additional stress constraint would have been allocated to that design element.

An additional simplifying assumption is that the stress constraint for a region is dependent only upon those shape design variables related to the boundaries of that region. This dependency is extended to other design elements through design variable linking. This assumption reduces considerably the computation necessary to obtain a stress gradient. Although it was recognized that this assumption is restrictive, it worked well for the test problems that follow. For global-type constraints, i.e., displacements and frequencies, no such assumption was imposed.

Applications

Some two-dimensional examples will be presented to demonstrate the shape design capability, although it should be mentioned that the techniques described in this paper are generally applicable to more complicated three-dimensional plate bending problems subjected to frequency as well as static loading conditions.

Shape and Location of Holes

The flat plate shown in Fig. 3a is 20×10 cm with an in-plane, uniformly varying tensile load applied at the ends in the global x -coordinate direction. Eight shape design elements were used to model two holes of size and location given in Table 1. The generated finite element mesh, shown in Fig. 3b, was composed of 768 constant strain triangles. The maximum stress for the initial design, shown in Fig. 3c, occurred at point

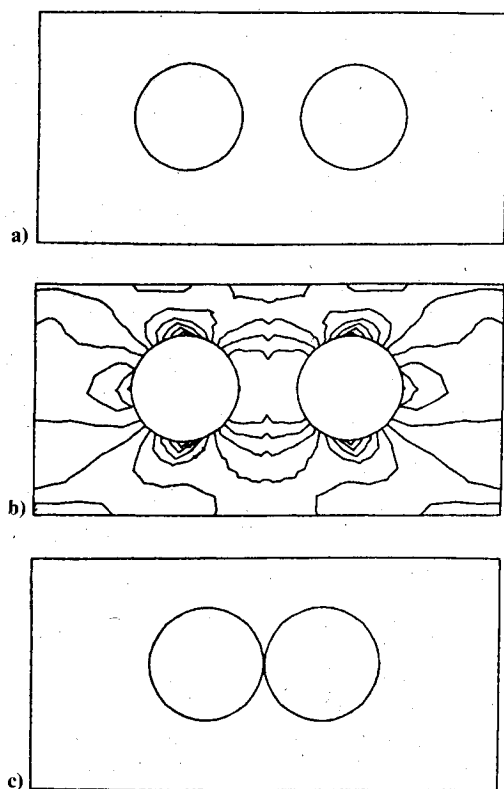


Fig. 5 a) Radius plus translation variables, case B; b) stress contours, case B (mass = 0.3939 kg); c) undesirable hole design.

A. The plate is considered to have a fixed, constant thickness of 0.3 cm with a stress constraint of 6500 N/cm^2 .

Several alternative designs, each having a different number of design variables, are shown with the corresponding stress contours in Figs. 4-7 and tabulated in Table 1. The design shown in Fig. 4a resulted from allowing only the radii of the holes to vary. Since the hole on the right side was "against" the stress constraint initially, only the hole on the left could become larger. Its size increased until it also was "against" the constraint. Figure 5a shows the results of allowing the holes to translate. The hole on the right is now permitted to increase in size as it "pushes" away from the constraint toward a region of lower stress. Finally, Fig. 6a shows the results of allowing the shape of the holes to vary using an elliptical shape function. In this case, the holes were permitted to elongate into the lowly stressed regions and at the same time change the degree of curvature on the side where the stress constraint was active. This curvature change reduced the stress, thus permitting an additional elongation in this direction. The holes also tended to move closer together. This movement, however, was restricted by side constraints in order to keep a reasonable amount of material around the edges. Figure 5c shows an obviously unrealistic design in which there were no side constraints. It does suggest, however, the necessity for a capability to completely redefine the design elements, as shown in Fig. 7a, based upon recognition that the material between the holes is being eliminated. This is not presently an automatic feature of the design technique but, due to the small amount of data required for defining the design elements, such a transition from holes to a slot was accomplished with very little effort. Figure 7b gives the optimum slot design which resulted in the lowest mass of all the alternative configurations.

Extended Problem with Displacement Constraints

Figure 8a represents a proposed design for an automotive rear suspension torque arm. It is approximately $50 \times 9 \text{ cm}$ and is 0.3 cm thick. For this example, a single, nonsymmetric,

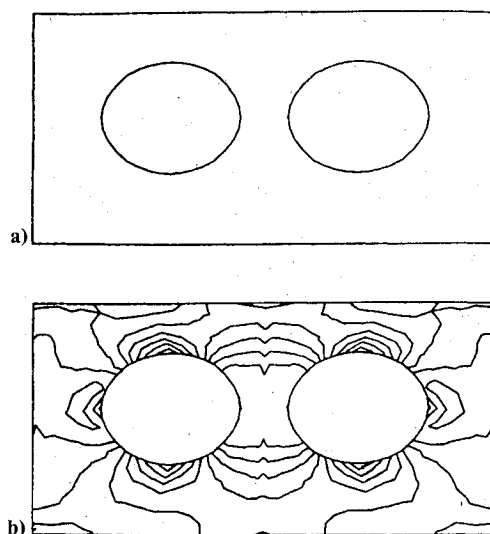


Fig. 6 a) Ellipse plus translation variables, case C (mass = 0.3655 kg); b) stress contours, case C.

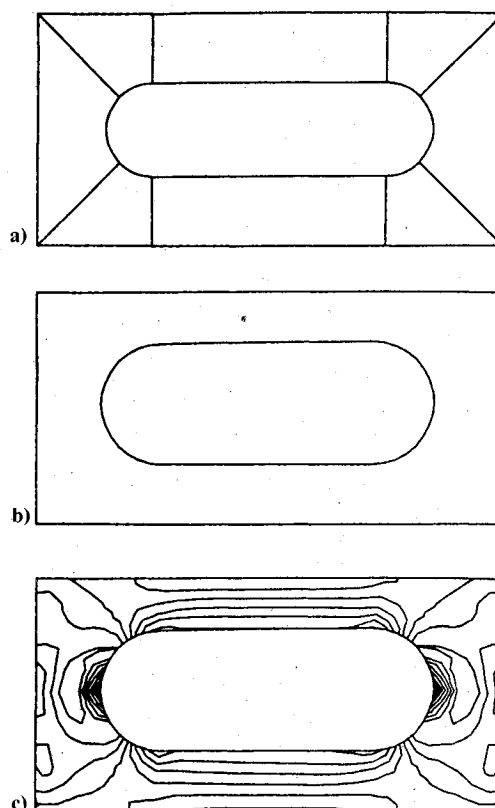


Fig. 7 a) Slot design element model, case D; b) final slot design (mass = 0.3091 kg); c) stress contours, case D.

static loading condition was applied in the x-y plane as shown in Fig. 8a. The arm was constrained against translation and rotation at four points around the hole at the right end. For the shape optimization, constraints were imposed upon stresses and the tip displacement of $81,000 \text{ N/cm}^2$ and 0.6 cm, respectively. The part was assumed to be at the optimum uniform thickness. Two configurations were chosen for comparison, one in which material was to be removed from exterior boundaries and one in which material was to be removed from the interior. The respective shape design element models are shown in Figs. 8a and 8c. The automatically generated finite element meshes for each configuration are shown in Figs. 8b and 8d.

The design variables for the configuration in Fig. 8b were chosen to permit material to be removed from the boundary between points A and B and to allow the hole on the right to vary. Two different shape functions were chosen for comparison. Figure 9 shows the shape functions, each having two design variables, A_1 and A_2 , which permit nonsymmetric boundary movements. Function A is a continuous cubic with zero slope at the ends. The design variables are the magnitude and location of the maximum value of the function. Function B is composed of discontinuous segments; cubic segments at the extremes connected by a linear segment. The design variables are the values of the function at the ends of the linear segment located at points C and D in Fig. 8b. The final boundary shape designs are shown in Figs. 10a and 10b, and Table 2 gives the final values of the design variables and the final masses. The superscripts in Table 2 refer to the particular boundary of the model and the subscripts refer to the particular design variable as shown in Fig. 9. Superscript 1 refers to the top of the model as viewed in Fig. 8a and superscript 2 refers to the bottom of the model. The boundary shape design using function B produced the lowest mass primarily due to the ability to remove more material from the lowly stressed areas. This is an extension of the design variable selection problem described earlier in which the character of the shape function has a marked effect on the final design. The effect can be thought of as an implicit

linking of the nodal coordinates which limits the amount of material which may be removed.

The configuration shown in Fig. 8c was chosen for comparison because of its possible efficiency in meeting the tip displacement design criterion. The design variables are the radii and location of the circular ends of the slot as well as the radius of the hole on the right. The final design is shown in Fig. 10c and the design variables are given in Table 2. The subscripts in the table refer to the radii as viewed from left to right. As expected, this configuration produced the lowest mass. There is a possibility, however, that this may not be a realistic design due to the long, narrow segment in compression. A more realistic comparison of the two configurations could be made by also considering the buckling capacity of each. For the constraints imposed, however, the slot design is the most mass efficient.

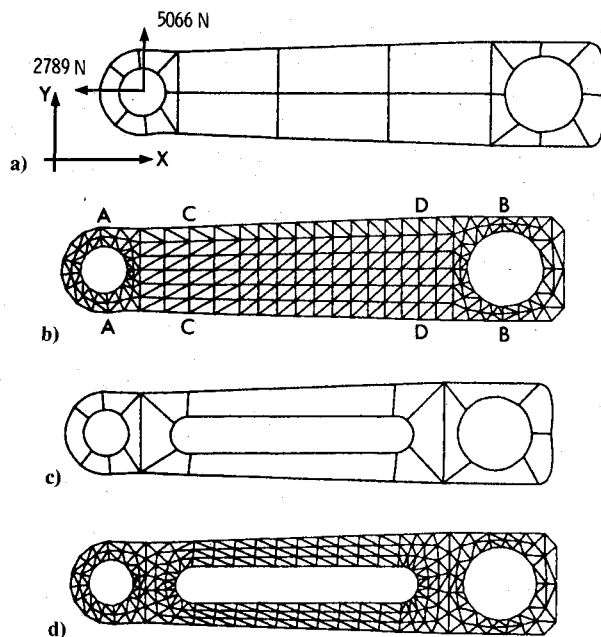


Fig. 8 a) Torque arm design element model; b) generated finite element model; c) slot design element model; d) generated finite element model.

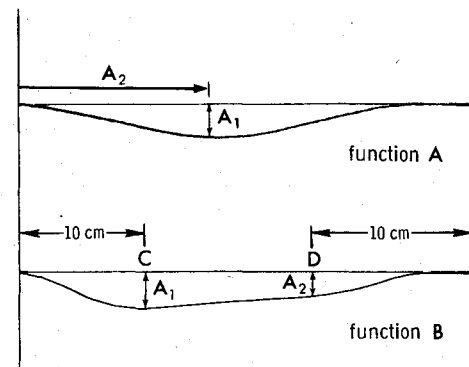


Fig. 9 Shape functions used in boundary design.

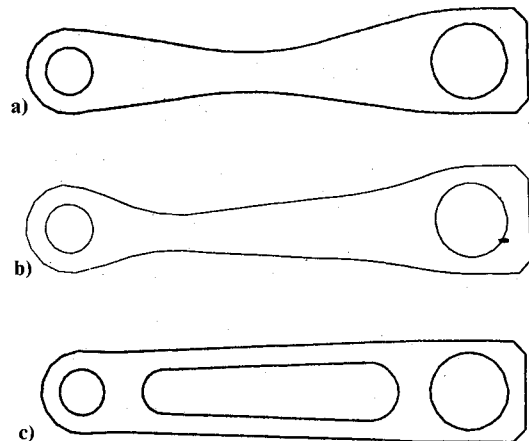


Fig. 10 a) Final boundary design using function A (mass = 0.7584 kg); b) final boundary design using function B (mass = 0.7091 kg); c) final slot design (mass = 0.6740 kg).

Table 2 Design results for automotive torque arm

Case	A_1^1	A_2^1	A_1^2	A_2^2	R	Mass, kg	Change, %		
Initial boundary	4.00	4.00	4.00	4.00	4.00	1.0300	0		
Boundary function A	7.44	3.92	1.88	4.31	3.94	0.7584	26.4		
Boundary function B	6.21	7.54	1.92	2.67	3.79	0.7091	31.1		
	R_1	X_1	Y_1	R_2	X_1	Y_1	R_3	Mass, kg	Change, %
Initial slot	2.0	335.84	34.85	2.0	357.72	32.56	4.00	0.7968	22.6
Final slot	2.386	335.84	35.07	3.161	357.72	32.68	4.221	0.6740	34.6

Summary and Conclusions

1) An optimization capability for shape design has been presented for general plate problems. The objective is mass reduction in which constraints can be imposed upon displacements, stresses, and frequencies. The finite element analysis technique can handle general three-dimensional plate and shell problems using a three-noded triangular plate element with combined stretching and bending characteristics. Although no examples have been presented, this technique should be capable of handling general three-dimensional shell design problems.

2) Shape design can be effectively incorporated in the design process by choosing variables which are the amplitudes of predetermined shape functions. This tends to allow fewer design variables but causes the choice of shape function to have a significant effect on the final mass.

3) A regionalized design element concept has been formulated which incorporates a number of features for facilitating the shape design process: a) the shape design variables control the boundaries of the element; b) the internal finite element mesh is automatically generated at the beginning of the design process, and the nodal points are regenerated at each design step; c) the number of stress constraints is greatly reduced by assigning one per shape design element; and d) the stress constraints can be considered to be dependent only upon the shape variables for that design element.

References

¹Zienkiewicz, O. C. and Campbell, J. S., "Shape Optimization and Sequential Linear Programming," *Optimum Structure Design*, edited by R. H. Gallagher and O. C. Zienkiewicz, John Wiley & Sons, New York, 1973, Chap. 7.

²Ramakrishnan, C. V. and Francavilla, A., "Structural Shape Optimization Using Penalty Function," *Journal of Structural Mechanics*, Vol. 3, No. 4, 1974-1975, pp. 403-422.

³Vitiello, E., "Shape Optimization Using Mathematical Programming and Modelling Techniques," *2nd Symposium on Structural Optimization*, AGARD CP-123, April 1973.

⁴Francavilla, A., Ramakrishnan, C. V., and Zienkiewicz, O. C., "Optimization of Shape to Minimize Stress Concentration," *Journal of Strain Analysis*, Vol. 10, No. 2, 1975, pp. 63-70.

⁵Kristensen, E. S. and Madsen, N. F., "On the Optimum Shape of Fillets in Plates Subjected to Multiple In-plane Loading Cases," *International Journal of Numerical Methods in Engineering*, Vol. 10, 1976, pp. 1007-1019.

⁶Dems, K. and Mroz, Z., "Multiparameter Structural Shape Optimization by the Finite Element Method," *International Journal of Numerical Methods in Engineering*, Vol. 13, 1978, pp. 247-263.

⁷Schnack, E., "An Optimization Procedure for Stress Concentration by the Finite Element Technique," *International Journal of Numerical Methods in Engineering*, Vol. 14, 1979, pp. 115-124.

⁸Bennett, J. A. and Nelson, M. F., "An Optimization Capability for Automotive Structures," *SAE Transactions*, Vol. 88, 1979, pp. 3236-3244.

⁹Fox, R. L., *Optimization Methods for Engineering Design*, Addison-Wesley Publishing Co., Inc., Reading, Mass., 1971, Chaps. 4 and 5.

¹⁰Schmit, L. A. and Miura, H., "A New Structural Analysis/Synthesis Capability—ACCESS 1," *AIAA Journal*, Vol. 14, May 1976, pp. 661-671.

¹¹DeRocher, L. L. and Gasper, A., "A Versatile Two-Dimensional Mesh Generator with Automatic Bandwidth Reduction," *Computers & Structures*, Vol. 10, 1979, pp. 561-575.

¹²Zienkiewicz, O. C., *The Finite Element Method in Engineering Science*, 3rd Ed., McGraw-Hill Book Co., London, 1977.

From the AIAA Progress in Astronautics and Aeronautics Series...

EXPERIMENTAL DIAGNOSTICS IN GAS PHASE COMBUSTION SYSTEMS—v. 53

Editor: Ben T. Zinn; Associate Editors: Craig T. Bowman, Daniel L. Hartley, Edward W. Price, and James F. Skifstad

Our scientific understanding of combustion systems has progressed in the past only as rapidly as penetrating experimental techniques were discovered to clarify the details of the elemental processes of such systems. Prior to 1950, existing understanding about the nature of flame and combustion systems centered in the field of chemical kinetics and thermodynamics. This situation is not surprising since the relatively advanced states of these areas could be directly related to earlier developments by chemists in experimental chemical kinetics. However, modern problems in combustion are not simple ones, and they involve much more than chemistry. The important problems of today often involve nonsteady phenomena, diffusional processes among initially unmixed reactants, and heterogeneous solid-liquid-gas reactions. To clarify the innermost details of such complex systems required the development of new experimental tools. Advances in the development of novel methods have been made steadily during the twenty-five years since 1950, based in large measure on fortuitous advances in the physical sciences occurring at the same time. The diagnostic methods described in this volume—and the methods to be presented in a second volume on combustion experimentation now in preparation—were largely undeveloped a decade ago. These powerful methods make possible a far deeper understanding of the complex processes of combustion than we had thought possible only a short time ago. This book has been planned as a means of disseminating to a wide audience of research and development engineers the techniques that had heretofore been known mainly to specialists.

671 pp., 6x9, illus., \$20.00 Member \$37.00 List

TO ORDER WRITE: Publications Dept., AIAA, 1290 Avenue of the Americas, New York, N.Y. 10019